arXiv:1701.03742v1 [cond-mat.mtrl-sci] 13 Jan 2017

Optical properties of dielectric plates coated with gapped graphene

G. L. Klimchitskaya[1,2] and V. M. Mostepanenko[1,2,3]

[1]*Central Astronomical Observatory at Pulkovo of the Russian Academy of Sciences, Saint Petersburg, 196140, Russia*

[2]*Institute of Physics, Nanotechnology and Telecommunications, Peter the Great Saint Petersburg Polytechnic University, St.Petersburg, 195251, Russia*

[3]*Kazan Federal University, Kazan, 420008, Russia*

Abstract

The optical properties of dielectric plates coated with gapped graphene are investigated on the basis of first principles of quantum electrodynamics. The reflection coefficients and reflectivities of graphene-coated plates are expressed in terms of the polarization tensor of gapped graphene and the dielectric permittivity of plate material. Simple approximate expressions for the required combinations of components of the polarization tensor applicable in the wide frequency region, where the presence of a gap influences the optical properties, are found. Numerical computations of the reflectivities of graphene-coated SiO_2 plates are performed for different values of the mass-gap parameter at different temperatures. It is shown that with an increasing gap width the reflectivity of a graphene-coated plate at the normal incidence decreases by up to a factor of 8 depending on the values of frequency and mass-gap parameter. The angle dependences of reflectivities for both polarizations of the incident electromagnetic waves have been computed for Si and SiO_2 plates coated with gapped graphene. We demonstrate that the TM reflectivity has a minimum value at some angle of incidence depending on the mass-gap parameter, frequency and temperature, whereas the TE reflectivity depends on the angle of incidence monotonously. However, for the graphene coatings with a nonzero mass-gap parameter the reflected light cannot be fully polarized. Possible applications of the obtained results are discussed.

PACS numbers: 12.20.Ds, 42.50.Ct, 78.20.Ci, 78.67.Wj

I. INTRODUCTION

Graphene is one of the family of two-dimensional materials possessing unusual optical, electrical and mechanical properties of much interest for both fundamental physics and applications in nanotechnology [1]. This is because at low energies the electronic excitations in graphene are described not by the Schrödinger equation but by the relativistic Dirac equation, where the speed of light c is replaced with the Fermi velocity $v_F \approx c/300$. It has been demonstrated [2, 3] that in the region of visible light the transparency and electrical conductivity of graphene are defined via the fundamental physical constants $\alpha = e^2/(\hbar c)$ and $e^2/(4\hbar)$, respectively. This was interpreted theoretically using the transport theory, current-current correlation functions, and the Kubo formula (see Refs. [4–6] for a review).

The electrical conductivity of graphene calculated within the cited approaches has been used to find the reflection coefficients and reflectivities of graphene with zero mass-gap parameter $\Delta = 2mc^2$, where m is the mass of electronic excitations [7, 8]. In so doing, the case of transverse magnetic (TM, i.e., p-polarized) electromagnetic waves was considered. Here, it is pertinent to note that for a pure (pristine) graphene $\Delta = m = 0$, but under the influence of defects of the structure, electron-electron interaction, and for graphene deposited on a substrate electronic excitations acquire some nonzero mass [9–13]. Usually the values of the mass-gap parameter are estimated as $\Delta \leqslant 0.1$ or 0.2 eV.

On the basis of first principles of quantum electrodynamics, one can express both the reflectivity and conductivity of graphene via the polarization tensor in (2+1)-dimensional space-time. For graphene this tensor was found at zero [14] and nonzero [15] temperature for the values of frequency restricted to only pure imaginary Matsubara frequencies. Note that in the framework of (2+1)-dimensional quantum electrodynamics with no relation to graphene the polarization tensor was studied long ago, e.g., in Refs. [16, 17]. The results of Refs. [14, 15] were applied to investigate the Casimir force in graphene systems in the framework of the Lifshitz theory [18–23] (previous calculations on this subject have been made using the density-density correlation functions, model dielectric permittivities of graphene and other methods [24–29]).

It is pertinent to note that the Lifshitz theory of the van der Waals and Casimir forces uses the reflection coefficients of interacting surfaces at pure imaginary Matsubara frequencies [30]. For calculation of the optical and conductivity properties of graphene, an analytic

continuation of the polarization tensor to real frequency axis is required. Such a continuation was found in Ref. [31] and used to study the reflectivity properties of pure graphene at any temperature over the wide frequency region on the basis of first principles of quantum electrodynamics. In Ref. [32] the same formalism was applied to investigate the electrical conductivity of pure graphene. Finally, in Ref. [33] an explicit representation for the polarization tensor of gapped graphene along the real frequency axis has been obtained and used for investigation of its reflectivity properties [33] and electrical conductivity [34]. It was shown that a nonzero mass of electronic excitations has a profound effect on the reflectivity of graphene at both zero and nonzero temperature [33]. Specifically, at zero temperature the reflectivities of gapped graphene go to zero with vanishing temperature, whereas for a gapless graphene in this limiting case the reflectivities go to a nonzero constant depending only on α and on the angle of incidence. At nonzero temperature, in contrast to the gapless case, the reflectivities of gapped graphene drop to zero in the vicinity of some fixed frequency [33].

Dielectric plates coated with graphene are used in many technological applications, such as the optical detectors [35], solar cells [36], transparent electrods [37], corrosium protection [38], optical biosensors [39], optoelectronic switches [40], and many others. The reflection coefficients for material plates coated with graphene were obtained in Ref. [41] in the random phase approximation. The exact expressions for both the TM and TE (i.e., for s-polarized electromagnetic waves) reflection coefficients of graphene-coated plates, where the plate material is described by the frequency-dependent dielectric permittivity and graphene by the polarization tensor, are derived in Ref. [22]. In Ref. [42] these reflection coefficients have been used to investigate the reflectivity properties of material plates coated with the pure (gapless) graphene. It was shown that at frequencies much smaller than the thermal frequency the coating with gapless graphene results in a pronounced (up to an order of magnitude) increase in the reflectivity of dielectric plates. At high frequencies (for metallic plates at all frequencies) the influence of graphene coating on the reflectivity properties was shown to be rather moderate [42].

In this paper, we investigate the optical properties of dielectric plates coated with gapped graphene on the basis of first principles of quantum electrodynamics. For this purpose, graphene coating is described by the polarization tensor with a nonzero mass-gap parameter in the form derived in Ref. [33], whereas the plate material is described by its dielectric

permittivity. The analytic expressions for both the TM and TE reflection coefficients and reflectivities of dielectric plates coated with gapped graphene are presented at frequencies smaller than the thermal frequency, where the effect of graphene coating plays an important role.

Numerical computations are performed for SiO_2 plates which are of frequent use in experiments as substrates for graphene coating [43–46]. Specifically, we calculate the reflectivities at normal incidence of SiO_2 plates coated with graphene sheets with different values of the mass-gap parameter at different temperatures. It is shown that with an increasing gap width the reflectivity of a graphene-coated substrate decreases. This decrease may be in several times, as compared to the case of a coating with gapless graphene, depending on the values of frequency and mass-gap parameter. According to our results, an increase of the gap parameter plays qualitatively the same role as a decrease of temperature for dielectric plates coated with a gapless graphene. We have also computed the angle dependences for both the TM and TE reflectivities of graphene-coated plates. It is shown that the TM reflectivity has a minimum value at some angle of incidence, whereas the TE reflectivity depends on the angle of incidence monotonically. In so doing, for coatings with gapped graphene the full polarization of reflected light turns out to be impossible. The angle dependences are found not only for graphene-coated SiO_2 plates, but for the plates made of high-resistivity Si , which are also used as substrates for graphene coating [47].

The paper is organized as follows. In Sec. II, we present analytic expressions for the reflection coefficients of dielectric plates coated with gapped graphene in different frequency regions. Section III is devoted to the investigation of influence of a nonzero gap on the reflectivity of graphene-coated plates at normal incidence. In Sec. IV the influence of gapped graphene on the angle dependence of reflectivities is considered. Section V contains our conclusions and discussion.

II. REFLECTION COEFFICIENTS IN DIFFERENT FREQUENCY REGIONS

We consider thick dielectric plate (semispace) coated with the sheet of gapped graphene. The plate material is described by the frequency-dependent dielectric permittivity $\epsilon(\omega)$ and graphene by the polarization tensor $\Pi_{kn}(\omega,\theta_i)$, where θ_i is the angle of incidence and k,n=0,1,2, taking into account the nonzero gap parameter. The reflection coefficients of a

graphene-coated plate for two independent polarizations of the electromagnetic field defined at real frequencies are given by [42]

$$
\begin{aligned}
R^{(g,p)}_{\rm TM}(\omega,\theta_i)&=\frac{\varepsilon(\omega)\cos\theta_i-\sqrt{\varepsilon(\omega)-\sin^2\theta_i}\left[1-\tilde{\Pi}_{00}(\omega,\theta_i)\right]}{\varepsilon(\omega)\cos\theta_i+\sqrt{\varepsilon(\omega)-\sin^2\theta_i}\left[1+\tilde{\Pi}_{00}(\omega,\theta_i)\right]},\\
R^{(g,p)}_{\rm TE}(\omega,\theta_i)&=\frac{\cos\theta_i-\sqrt{\varepsilon(\omega)-\sin^2\theta_i}-\tilde{\Pi}(\omega,\theta_i)}{\cos\theta_i+\sqrt{\varepsilon(\omega)-\sin^2\theta_i}+\tilde{\Pi}(\omega,\theta_i)}.
\end{aligned}
\tag{1}
$$

Here, the quantities $\tilde{\Pi}_{00}$ and $\tilde{\Pi}$ are expressed via the polarization tensor of graphene in the following way:

$$
\begin{aligned}
\tilde{\Pi}_{00}(\omega,\theta_i)&=-\frac{ic}{\hbar\omega}\,\frac{\cos\theta_i}{\sin^2\theta_i}\,\Pi_{00}(\omega,\theta_i),\\
\tilde{\Pi}(\omega,\theta_i)&=\frac{ic^3}{\hbar\omega^3}\,\frac{1}{\sin^2\theta_i}\,\Pi(\omega,\theta_i),
\end{aligned}
\tag{2}
$$

where the quantity Π is defined as

$$
\Pi(\omega,\theta_i)=\frac{\omega^2}{c^2}[\sin^2\theta_i\Pi_{\rm tr}(\omega,\theta_i)+\cos^2\theta_i\Pi_{00}(\omega,\theta_i)] \tag{3}
$$

and $\Pi_{\rm tr}=\Pi^k_k$ is the trace of the polarization tensor.

The explicit exact formulas for the quantities Π_{00}, $\Pi_{\rm tr}$ and Π at real frequencies in the case of gapped graphene are presented in Ref. [33]. Here, we use only the approximate asymptotic representations for these formulas, which are quite sufficient to calculate the impact of nonzero mass-gap parameter on the reflectivity of graphene-coated plate. In particular, we omit the nonlocal contributions which are of the order of $v_F^2/c^2\sim 10^{-5}$.

We consider first the frequency region $\hbar\omega<\Delta$, where quantities Π_{00} and Π are real. Using Eq. (2) and the results for Π_{00} and Π obtained in Eqs. (5), (6), (30), and (56) of Ref. [33] one finds

$$
\begin{aligned}
\tilde{\Pi}_{00}(\omega,\theta_i)&\approx 2i\alpha\cos\theta_i\,\left[\Phi_1\left(\frac{\hbar\omega}{\Delta}\right)+\frac{4}{\nu}I(\mu,\nu)\right],\\
\tilde{\Pi}(\omega,\theta_i)&\approx\tilde{\Pi}(\omega)\approx 2i\alpha\,\left[\Phi_1\left(\frac{\hbar\omega}{\Delta}\right)+\frac{4}{\nu}I(\mu,\nu)\right],
\end{aligned}
\tag{4}
$$

where

$$
\begin{aligned}
\Phi_1(x)&=\frac{1}{x}-\left(1+\frac{1}{x^2}\right)\operatorname{arctanh}x,\\
I(\mu.\nu)&=\int_\mu^\infty\frac{dv}{e^v+1}\left(1+\frac{4\mu^2+\nu^2}{4v^2-\nu^2}\right)
\end{aligned}
\tag{5}
$$

and the following parameters are introduced:

$$\mu \equiv \frac{mc^2}{k_B T} = \frac{\Delta}{2k_B T}, \qquad \nu \equiv \frac{\hbar\omega}{k_B T}. \tag{6}$$

Note that, strictly speaking, Eq. (56) of Ref. [33] and, thus, Eq. (4) here, are defined under a more stringent condition $\hbar\omega \lesssim mc^2$. Computations show, however, that Eq. (4) actually leads to very small errors, as compared to the exact formulas, in a wider frequency region $\hbar\omega < 2mc^2 = \Delta$. Note also that both the exact formulas and the approximate expressions for $\tilde{\Pi}_{00}$ and $\tilde{\Pi}$ defined in Eq. (4) are characterized by two peculiarities. In the limiting case $\hbar\omega \to \Delta$ it holds $|\tilde{\Pi}_{00}|, |\tilde{\Pi}| \to \infty$ due to $|\Phi_1| \to \infty$. As a result, the absolute values of both reflection coefficients turn into unity over a nonphysically narrow frequency interval (see Ref. [33] for details). Furthermore, for some value of frequency $\hbar\omega_0 < \Delta$ it holds $\tilde{\Pi}_{00} = \tilde{\Pi} = 0$. According to Eq. (1), at $\omega = \omega_0$ graphene coating does not influence the reflectivity properties of a dielectric plate. At temperatures satisfying the condition $k_B T \lesssim mc^2$, the frequency ω_0 differs noticeably from $\Delta/\hbar$. This is, however, a frequency region, where the graphene coating has only a minor influence on the reflectivity properties of a plate (see Sec. III). Under a condition $mc^2 < k_B T$ the value of ω_0 belongs to a nonphysically narrow vicinity of the frequency $\hbar\omega = \Delta$. For very narrow gaps ($mc^2 \ll k_B T$), this case is further discussed in Sec. III.

Below, Eqs. (1) and (4)–(6) are used to calculate the TM and TE reflectivities of dielectric plates coated with gapped graphene

$$\begin{aligned} \mathcal{R}_{\rm TM}(\omega,\theta_i) &= |R_{\rm TM}(\omega,\theta_i)|^2, \\ \mathcal{R}_{\rm TE}(\omega,\theta_i) &= |R_{\rm TE}(\omega,\theta_i)|^2 \end{aligned} \tag{7}$$

in the frequency region $\hbar\omega < \Delta$. The computational results show that a pronounced impact of graphene coating on the reflectivity of dielectric plates occurs only under the condition $\hbar\omega \ll k_B T$ (see Ref. [42] for the case of a gapless graphene coating and Sec. III). Taking into account that at room temperature $k_B T \approx 0.026\,\text{eV}$, the frequency region $\hbar\omega \ll k_B T$ belongs to the area of application of Eq. (4), $\hbar\omega < \Delta$, with exception of only the case of graphene with very narrow gaps.

To study the influence of graphene with very small mass-gap parameter and the limiting transition to the case of gapless graphene, the analytic expressions for $\tilde{\Pi}_{00}$ and $\tilde{\Pi}$ in the frequency region $\hbar\omega \geq \Delta$ are also required in addition to Eq. (4). In accordance with the

above remark, it is sufficient to present them under the condition $\hbar\omega \ll k_BT$. We, thus, have $\Delta \leqslant \hbar\omega \ll k_BT$ or, using the notation (6), $\mu \ll 1$ and $\nu \ll 1$.

Under the conditions μ, $\nu \ll 1$ and $\hbar\omega \geqslant \Delta$ the quantities Π_{00} and Π are obtained in Eqs. (5)–(7) and (79) of Ref. [33] (note that the imaginary parts of Π_{00} and Π at $T = 0$ cancel with the leading contributions to the imaginary parts of thermal corrections to these quantities). As a result, using Eq. (2), one arrives at

$$\begin{aligned}
\tilde{\Pi}_{00}(\omega,\theta_i) &\approx 2i\alpha\cos\theta_i\left[\Phi_2\left(\frac{\Delta}{\hbar\omega}\right)+\frac{4}{\nu}\ln(1+e^{-\nu/2})\right],\\
\tilde{\Pi}(\omega) &\approx 2i\alpha\left[\Phi_2\left(\frac{\Delta}{\hbar\omega}\right)+\frac{4}{\nu}\ln(1+e^{-\nu/2})\right],
\end{aligned}
\tag{8}$$

where

$$\Phi_2(x) = x - \left(1+x^2\right)\operatorname{arctanh} x. \tag{9}$$

Using Eqs. (1) and (7)–(9), one can calculate the TM and TE reflectivities of a plate coated with gapped graphene in the frequency region $\Delta \leqslant \hbar\omega \ll k_BT$.

At not-too-high temperatures, as compared to room temperature, in the frequency region $\hbar\omega \ll k_BT$ the dielectric permittivities of dielectric materials are real and approximately equal to their static values $\varepsilon(\omega) \approx \varepsilon_0$. Taking into account that the quantities $\tilde{\Pi}_{00}$ and $\tilde{\Pi}$ in Eqs. (4) and (8) are pure imaginary and using Eq. (1), the reflectivities (7) can be expressed in the form

$$\begin{aligned}
\mathcal{R}_{\rm TM}(\omega,\theta_i) &= \frac{(\varepsilon_0\cos\theta_i-\sqrt{\varepsilon_0-\sin^2\theta_i})^2+(\varepsilon_0-\sin^2\theta_i)|\tilde{\Pi}_{00}(\omega,\theta_i)|^2}{(\varepsilon_0\cos\theta_i+\sqrt{\varepsilon_0-\sin^2\theta_i})^2+(\varepsilon_0-\sin^2\theta_i)|\tilde{\Pi}_{00}(\omega,\theta_i)|^2},\\
\mathcal{R}_{\rm TE}(\omega,\theta_i) &= \frac{(\cos\theta_i-\sqrt{\varepsilon_0-\sin^2\theta_i})^2+|\tilde{\Pi}(\omega,\theta_i)|^2}{(\cos\theta_i+\sqrt{\varepsilon_0-\sin^2\theta_i})^2+|\tilde{\Pi}(\omega,\theta_i)|^2}.
\end{aligned}
\tag{10}$$

At the normal incidence ($\theta_i = 0$) the TM and TE reflectivities coincide, as it should be.

Below these equations are used to examine the optical properties of dielectric plates coated with gapped graphene.

III. INFLUENCE OF GRAPHENE GAP ON THE REFLECTIVITY AT NORMAL INCIDENCE

In this section, we calculate the reflectivity properties of fused silica (SiO_2) plates coated with gapped graphene. As mentioned in Sec. I, SiO_2 plates are often used as substrates

for coating with graphene [43–46]. The static dielectric permittivity of SiO_2 is equal to $\varepsilon_0 \approx 3.82$. For SiO_2 the static value remains applicable for all frequencies $\hbar\omega < 10\,\mathrm{meV}$ [48]. At larger frequencies the optical data for $\varepsilon(\omega)$ should be used [48].

Numerical computations for the TM and TE reflectivities of SiO_2 plate coated with gapped graphene have been performed by Eqs. (4) and (10) in the frequency region from $10^{-3}\,\mathrm{meV}$ to $10\,\mathrm{meV}$. In this frequency region the same results were obtained using Eqs. (1), (4), and (7) in combination with the optical data for $\varepsilon(\omega)$, where they are available (i.e., at $\hbar\omega \geqslant 2.48\,\mathrm{meV}$ [48]). At higher frequencies ($\hbar\omega > 10\,\mathrm{meV}$) Eqs. (1), (4), and (7) should be used in computations up to $\hbar\omega = \Delta$. At these frequencies, however, there is no influence of either the gap parameter or the graphene coating by itself on the reflectivity properties of a plate.

In Fig. 1, the reflectivities of graphene-coated SiO_2 plates at the normal incidence are shown as functions of frequency at $T = 300\,\mathrm{K}$ by the solid lines 1, 2, and 3 for the mass-gap parameter equal to $\Delta = 0.2$, 0.1, and $0.02\,\mathrm{eV}$, respectively. In the same figure, the dashed line shows the reflectivity of a SiO_2 plate coated with a gapless graphene at the normal incidence. The lower solid line marked SiO_2 demonstrates the reflectivity of an uncoated plate, which is obtained from Eq. (10) at $\theta_i = 0$, $\tilde{\Pi}_{00} = \tilde{\Pi} = 0$

$$\mathcal{R}_{\mathrm{TM,TE}} = \left(\frac{\sqrt{\varepsilon_0}-1}{\sqrt{\varepsilon_0}+1}\right)^2. \tag{11}$$

In the region $\hbar\omega > 10\,\mathrm{meV}$ the frequency dependence of $\mathrm{Re}\,\varepsilon(\omega)$ and nonzero $\mathrm{Im}\,\varepsilon(\omega)$ are of some impact on the lower solid line.

As is seen in Fig. 1, the presence of a gap results in a significant decrease of the reflectivity of graphene-coated SiO_2 plate. This decrease is deeper for the larger mass-gap parameter. As an example, for $\Delta = 0.2\,\mathrm{eV}$ (which is a realistic width of the gap for graphene-coated substrates) the reflectivity of the plate coated with gapped graphene is smaller than that for a gapless graphene by up to a factor of 8 depending on the value of frequency. Comparing Fig. 1 with Fig. 3 of Ref. [42], where similar results for a gapless graphene are presented at different temperatures, one can conclude that increasing of the mass-gap parameter at fixed temperature produces qualitatively the same effect on the reflectivity as does decreasing temperature in the case of a coating with pure graphene.

From Fig. 1 one can see that the graphene coating ceases to influence the reflectivity of SiO_2 plate at $\hbar\omega < 10\,\mathrm{meV} < \Delta$ for all three values of the width gap considered. At the

same time, the values of frequency, where the influence of graphene coating is noticeable, are much smaller than the thermal frequency

$$\omega_T \equiv \frac{k_B T}{\hbar} = 26\,\mathrm{meV} = 3.9 \times 10^{13}\,\mathrm{rad/s} \tag{12}$$

at room temperature. This is in agreement with similar result for a coating made of pure graphene [42].

Note that for not too narrow gaps considered above it holds $\mu \sim 1$ or $\mu > 1$, whereas the inequality $\hbar\omega \ll k_B T$ means that $\nu \ll 1$. Then it follows also that $\hbar\omega \ll \Delta$. Expanding $\Phi_1(\hbar\omega/\Delta)$ defined in Eq. (5) in powers of the small parameter $\hbar\omega/\Delta$, one obtains

$$\Phi\left(\frac{\hbar\omega}{\Delta}\right) \approx -\frac{4}{3}\,\frac{\hbar\omega}{\Delta}. \tag{13}$$

If it also assumed that μ is sufficiently large (for instance, for $\Delta = 0.2\,\mathrm{eV}$ at $T = 300\,\mathrm{K}$ we have $\mu \approx 3.85$), we can neglect by unity, as compared to e^v in the definition of I in Eq. (5). Neglecting also by the small quantity ν^2 in comparison with $4\mu^2$ and $4v^2$, and calculating the integral in Eq. (5), one arrives at [33]

$$I(\mu, \nu) \approx 2e^{-\mu}. \tag{14}$$

Computations show that for graphene coating with $\Delta = 0.1\,\mathrm{eV}$ the use of Eq. (4) with the functions (13) and (14), rather than (5), leads to the same results plotted as line 1 in Fig. 1. For smaller Δ the more exact results are obtained by using Eqs. (4) and (5).

Note that two peculiar frequencies $\hbar\omega = \Delta$, where the reflectivity turns into unity, and $\hbar\omega_0 < \Delta$, where the graphene coating does not influence the reflectivity properties of a plate (see Sec. II) are not shown in Fig. 1 because they occur at higher frequencies (at 20 meV and at slightly smaller frequency, respectively, for the line 3 related to the case of the smallest mass-gap parameter). All these frequencies belong to the region of absorption bands of SiO_2, where the graphene coating does not make any impact on the reflectivity properties taking into account nonphysically small half-widths of the corresponding resonances [33].

To discuss the role of different values of temperature, in Fig. 2 we plot the reflectivities of graphene-coated SiO_2 plates at $T = 150\,\mathrm{K}$. The same notations for different lines, as in Fig. 1, are used. In the frequency region from 10^{-5} to 10 meV computations have been performed using Eqs. (4) and (10). As is seen in Fig. 2, the impact of graphene coating with different values of the mass-gap parameter is qualitatively the same. as in Fig. 1. One can

conclude, however, that at $T = 150\,\mathrm{K}$ the decrease of reflectivities down to the reflectivity of an uncoated SiO_2 plate starts at much lower frequencies than at $T = 300\,\mathrm{K}$. For example, for the line 1 ($\Delta = 0.2\,\mathrm{eV}$) this decrease starts at $\hbar\omega \approx 10^{-5}\,\mathrm{meV}$, whereas in Fig. 1 it starts at for orders of magnitude higher frequency. By and large, from the comparison of Fig. 2 and Fig. 1 it is seen that at $T = 150\,\mathrm{K}$ the impact of graphene coating with some fixed gap parameter on the reflectivity of SiO_2 plate in stronger than at $T = 300\,\mathrm{K}$.

In the end of this section, we calculate the reflectivity of a SiO_2 plate coated with gapped graphene at the normal incidence as a function of the quasiparticle mass at some fixed frequency, $\hbar\omega = 0.1\,\mathrm{meV}$, for instance. Computations are performed by using Eqs. (4) and (10) in the region of masses $2mc^2 = \Delta > \hbar\omega$ and by Eqs. (8) and (10) in the region $2mc^2 \leqslant \hbar\omega$. In Fig. 3 the computational results for the reflectivities are presented by the upper and lower solid lines computed at 300 and 150 K, respectively. The overlapping solid and dashed vertical lines demonstrate the narrow resonances which occur at $T = 300$ and $150\,\mathrm{K}$ under the condition $2mc^2 = \hbar\omega = 0.1\,\mathrm{meV}$.

As is seen in Fig. 3, for small masses below 0.1 meV there is no influence of the gap on the reflectivity of a graphene-coated SiO_2 plate. At $T = 150\,\mathrm{K}$ the gap comes into play at smaller width than at $T = 300\,\mathrm{K}$. As a result, the reflectivity of a graphene-coated plate drops to that of an uncoated graphene for $mc^2 \approx 65\,\mathrm{meV}$ at $T = 150\,\mathrm{K}$ and for $mc^2 \approx 140\,\mathrm{meV}$ at $T = 300\,\mathrm{K}$.

Quantitatively, from Fig. 3 at $T = 300\,\mathrm{K}$ one has $\mathcal{R}_{\mathrm{TM,TE}} = 0.934$ for $m = 0$ and 0.919 for $m = 0.01\,\mathrm{meV}$, i.e., the relative change of only 1.6%. At $T = 150\,\mathrm{K}$ one obtains $\mathcal{R}_{\mathrm{TM,TE}} = 0.784$ for $m = 0$ and 0.662 for $m = 0.01\,\mathrm{meV}$. This corresponds to a much larger relative change of 18.4%. Thus, at lower temperature the graphene coating with the same gap produces a larger relative impact on the reflectivity, as compared to the case of gapless graphene, in accordance with a conclusion made from the comparison of Figs. 1 and 2.

IV. INFLUENCE OF GRAPHENE COATING ON THE ANGLE DEPENDENCE OF REFLECTIVITIES

Here, we consider the angle dependences of both TM and TE reflectivities of dielectric plates coated with gapped graphene with different values of the mass-gap parameter. Computations are performed at $T = 300\,\mathrm{K}$ by using Eqs. (4) and (10), i.e., in the region, where

the nonzero gap makes an important impact on the reflectivity properties of graphene-coated plates.

In Fig. 4(a) the TM reflectivities of SiO_2 plates with no graphene coating and coated by graphene with $\Delta = 0.2$, 0.15, 0.1, and $\leqslant 0.02\,\mathrm{eV}$ are shown at $\hbar\omega = 0.1\,\mathrm{eV}$ as functions of the incidence angle by the five solid lines from bottom to top, respectively. In Fig. 4(b) similar computational results for the TE reflectivity are presented.

As is seen in Fig. 4(a), the most pronounced influence of graphene coating on the TM reflectivity is for a gapless or having a narrow gap $\Delta \leqslant 0.02\,\mathrm{eV}$ graphene (the upper line). With increasing width of the gap, the reflectivity becomes smaller, preserving the character of an angle dependence with a typical minimum value which shifts to smaller angles of incidence. Only for an uncoated SiO_2 plate (the lowest line) the TM reflectivity takes zero value at the Brewster angle $\theta_B = 62.90^\circ$. In this case the reflected light is fully (TE) polarized. Note that at much higher frequencies the full polarization of reflected light is possible also for a SiO_2 plate coated with gapless graphene [42]. In this frequency region, however, the presence of nonzero gap does not influence the reflectivity properties of graphene-coated plate.

From Fig. 4(b) it is seen that the TE reflectivities of graphene-coated SiO_2 plates also decrease with increasing Δ at any angle of incidence. Unlike Fig. 4(a), however, the TE reflectivities decrease monotonously with decreasing angle of incidence.

To investigate the role of material properties of a substrate, similar computations of angle dependences of the reflectivities have been performed for graphene-coated plates made of high-resistivity Si. This material possesses much higher static dielectric permittivity $\varepsilon_0 = 11.67$ [48]. The computational results obtained using Eqs. (4) and (10) are presented in Fig. 5 using the same notations and the same values of all parameters as in Fig. 4.

As is seen in Fig. 5(a,b), the dependences of both TM and TE reflectivities of Si plates coated with gapped graphene are qualitatively the same as for graphene-coated SiO_2 plates [see Fig. 4(a,b)]. Specifically, the Brewster angle $\theta_B = 73.68^\circ$ is achieved for only an uncoated Si plate. It is seen, however, that for both TM and TE reflectivities the two lowest lines (related to the cases of an uncoated plate and of a plate coated by graphene with $\Delta = 0.2\,\mathrm{eV}$) are overlapping. This means that coating by graphene with relatively wide gap does not make a dramatic effect on the angle dependences of reflectivities of plates with large ε_0.

It is interesting to investigate a dependence of the angle θ_0, where the minimum TM

reflectivity of graphene-coated plate is achieved [see Figs. 4(a) and 5(a)], on the quasiparticle mass m for different plate materials at different temperatures. From the first equality in Eq. (10) one concludes that the quantity

$$F(\omega) \equiv \frac{|\tilde{\Pi}_{00}(\omega, \theta_i)|}{\cos\theta_i} \tag{15}$$

does not depend on the angle of incidence. Then, from the first equality in Eq. (10), it is easily seen that the minimum value of the quantity $\mathcal{R}_{\rm TM}$ is achieved at the angle of incidence $\theta_i = \theta_0$ satisfying the following equation:

$$\cos^6\theta_0 + \frac{3(\varepsilon_0 - 1)}{2}\cos^4\theta_0 \tag{16}$$

$$+\frac{(\varepsilon_0 - 1)^2[\varepsilon_0 + 1 + F^2(\omega)]}{2F^2(\omega)}\cos^2\theta_0 - \frac{(\varepsilon_0 - 1)^2}{2F^2(\omega)} = 0. \tag{17}$$

This equation has only one solution for $\cos^2\theta_0$ satisfying the condition

$$0 \leqslant \cos^2\theta_0 \leqslant 1. \tag{18}$$

In Fig. 6 we present computational results for the angle θ_0, as a function of the quasiparticle mass m, obtained by solving Eq. (16). The pair of two upper lines is plotted at $T = 300\,\mathrm{K}$, $\hbar\omega = 0.1\,\mathrm{meV}$ for Si and SiO_2 plates from top to bottom, respectively. The pair of two lower lines is plotted at $T = 150\,\mathrm{K}$, $\hbar\omega = 0.1\,\mathrm{meV}$ for the same materials in the same sequence. As is seen in Fig. 6, at small masses (narrow gaps) the values of θ_0 depend only on the temperature and are almost independent on the plate material. After some transition region of masses, where both the value of temperature and material properties influence the result, the value of θ_0 is coming to depend of only on the plate material. Specifically, for SiO_2 plate at $T = 300\,\mathrm{K}$ the angle θ_0 is equal to 89.48° for a gapless graphene coating and takes the values 84.35° and 63.19° for gapped graphene coatings with $m = 0.05$ and $0.1\,\mathrm{eV}$, respectively. For graphene-coated Si plate at the same temperature one has $\theta_0 = 89.48^\circ$, 84.54°, and 73.74° $m = 0$, 0.05, and $0.1\,\mathrm{eV}$, respectively. At $T = 150\,\mathrm{K}$ for the same respective values of m the angle θ_0 is equal to 87.90°, 62.92°, and 62.90° for SiO_2 and 87.90°, 73.69°, and 73.68° for Si plate. As is seen in Fig. 6, for the plate materials with larger ε_0, the value of θ_0 becomes mass-independent for smaller values of the mass-gap parameter of graphene. One can also see that this property is preserved at any temperature.

V. CONCLUSIONS AND DISCUSSION

In this paper, we have investigated the optical properties of dielectric plates coated with gapped graphene on the basis of first principles of quantum electrodynamics. For this purpose, graphene was described by the polarization tensor with a nonzero mass-gap parameter defined along the real frequency axis at any temperature, whereas the plate material was characterized by its dielectric permittivity. Simple approximate expressions for the polarization tensor and for the transverse magnetic and transverse electric reflectivities of graphene-coated plates have been derived. These expression are valid for all frequencies smaller than the width of the gap, where the mass-gap parameter makes a major impact on the reflectivities, and also for frequencies exceeding the width of the gap (the latter under a condition that they are much smaller than the thermal frequency).

The obtained expressions have been applied to calculate an impact of the mass-gap parameter on the reflectivity of graphene-coated SiO_2 plates at the normal incidence at different temperatures. It is shown that at fixed frequency the reflectivity of graphene-coated plates decreases with increasing mass-gap parameter. Calculations show that for a wider gap the reflectivity begins its decreasing from unity to the reflectivity of an uncoated SiO_2 plate at lower frequency. For the gap width Δ=0.02 eV at T=300K the reflectivities of plates coated with gapped and gapless graphene are shown to be rather close. At the same time, the reflectivity of SiO_2 plate coated with gapped graphene with Δ=0.2 eV may be smaller by up to a factor of 8 than the reflectivity of a plate coated with gapless graphene. Qualitatively the dependences of reflectivities on frequency are akin in the cases of graphene coatings with different values of the mass-gap parameter and a gapless graphene coating at different temperatures. The dependence of a reflectivity on the quasiparticle mass m is also computed over the wide range of mc^2 from 10^{-2} meV to 100 meV at different temperatures.

Furthermore, the obtained expressions have been used to calculate the angle dependences of the TM and TE reflectivities of SiO_2 and Si plates coated with gapped graphene with different values of the mass-gap parameter. It was shown that the TM reflectivity has a minimum value at some incidence angle θ_0, which depends on the mass-gap parameter of graphene coating. These minimum values, however, are always larger than zero. Thus, the reflected light from a plate coated with gapped graphene cannot be fully polarized. This is different from the coating with a gapless graphene where the full (TE) polarization of

reflected light is possible at high frequencies. We have also calculated the dependence of an angle θ_0 on the mass-gap parameter for both SiO_2 and Si plates at different temperatures. It is shown that θ_0 decreases with increasing mass-gap parameter and that the limiting values of θ_0 at large m do not depend on the temperature, but only on the plate material.

The above results demonstrate that a nonzero gap of graphene has profound effects on the optical properties of graphene-coated dielectric plates, which should be taken into account in numerous applications, such as the optical detectors, solar cells, optoelectronic switches and others mentioned in Sec. I. In Sec. I it was also discussed that a nonzero gap arises under the influence of different factors including the defects of structure or impurities. A more full account of the role of impurities can be made by considering nonzero chemical potential. A rough estimate [49] shows that the above results obtained for zero chemical potential can be valid for the concentration of impurities below $1.2\times10^{10}\,\mathrm{cm}^{-2}$. In this respect further generalization of the developed formalism, e.g., for the case of graphene coatings with nonzero chemical potential [50] is of interest for future work.

Acknowledgments

The work of V.M.M. was partially supported by the Russian Government Program of Competitive Growth of Kazan Federal University.

[1] M. I. Katsnelson, *Graphene: Carbon in Two Dimensions* (Cambridge University Press, Cambridge, 2012).

[2] R. R. Nair, P. Blake, A. N. Grigorenko, K. S. Novoselov, T. J. Booth, T. Stauber, N. M. R. Peres, and A. K. Geim, Science **320**, 1308 (2008).

[3] A. B. Kuzmenko, E. van Neumen, F. Carbone, and D. van der Marel, Phys. Rev. Lett. **100**, 117401 (2008).

[4] V. P. Gusynin, S. G. Sharapov, and J. P. Carbotte, Int. J. Mod. Phys. B **21**, 4611 (2007).

[5] N. M. R. Peres, Rev. Mod. Phys. **82**, 2673 (2010).

[6] S. Das Sarma, S. Adam, E. H. Hwang, and E. Rossi, Rev. Mod. Phys. **83**, 407 (2011).

[7] L. A. Falkovsky and S. S. Pershoguba, Phys. Rev. B **76**, 153410 (2007).

[8] T. Stauber, N. M. R. Peres, and A. K. Geim, Phys. Rev. B **78**, 085432 (2008).

[9] S. A. Jafari, J. Phys.: Condens. Matter **24**, 205802 (2012).

[10] P. K. Pyatkovsky, J. Phys.: Condens. Matter **21**, 025506 (2009).

[11] V. P. Gusynin, S. G. Sharapov, and J. P. Carbotte, New J. Phys. **11**, 095013 (2009).

[12] V. P. Gusynin and S. G. Sharapov, Phys. Rev. B **73**, 245411 (2006).

[13] T. Takahashi, K. Sugawara, E. Noguchi, T. Sato, and T. Takahashi, Carbon **73**, 141 (2014).

[14] M. Bordag, I. V. Fialkovsky, D. M. Gitman, and D. V. Vassilevich, Phys. Rev. B **80**, 245406 (2009).

[15] I. V. Fialkovsky, V. N. Marachevsky, and D. V. Vassilevich, Phys. Rev. B **84**, 035446 (2011).

[16] T. W. Appelquist, M. J. Bowick, D. Karabali, and L. C. R. Wijewardhana, Phys. Rev. D **33**, 3704 (1986).

[17] N. Dorey and N. E. Mavromatos, Nucl. Phys. B **386**. 614 (1992).

[18] M. Bordag, G. L. Klimchitskaya, and V. M. Mostepanenko, Phys. Rev. B **86**, 165429 (2012).

[19] M. Chaichian, G. L. Klimchitskaya, V. M. Mostepanenko, and A. Tureanu, Phys. Rev. A **86**, 012515 (2012).

[20] G. L. Klimchitskaya and V. M. Mostepanenko, Phys. Rev. B **87**, 075439 (2013).

[21] G. L. Klimchitskaya, V. M. Mostepanenko, and Bo E. Sernelius, Phys. Rev. B **89**, 125407 (2014).

[22] G. L. Klimchitskaya, U. Mohideen, and V. M. Mostepanenko, Phys. Rev B **89**, 115419 (2014).

[23] G. L. Klimchitskaya and V. M. Mostepanenko, Phys. Rev B **91**, 174501 (2015).

[24] G. Gómez-Santos, Phys. Rev. B **80**, 245424 (2009).

[25] D. Drosdoff and L. M. Woods, Phys. Rev. B **82**, 155459 (2010).

[26] D. Drosdoff and L. M. Woods, Phys. Rev. A **84**, 062501 (2011).

[27] Bo E. Sernelius, Europhys. Lett. **95**, 57003 (2011).

[28] Bo E. Sernelius, Phys. Rev. B **85**, 195427 (2012).

[29] A. D. Phan, L. M. Woods, D. Drosdoff, I. V. Bondarev, and N. A. Viet, Appl. Phys. Lett. **101**, 113118 (2012).

[30] G. L. Klimchitskaya, U. Mohideen, and V. M. Mostepanenko, Rev. Mod. Phys. **81**, 1827 (2009).

[31] M. Bordag, G. L. Klimchitskaya, V. M. Mostepanenko, and V. M. Petrov, Phys. Rev. D **91**, 045037 (2015); **93**, 089907(E) (2016).

[32] G. L. Klimchitskaya and V. M. Mostepanenko, Phys. Rev B **93**, 245419 (2016).

[33] G. L. Klimchitskaya and V. M. Mostepanenko, Phys. Rev A **93**, 052106 (2016).

[34] G. L. Klimchitskaya and V. M. Mostepanenko, Phys. Rev B **94**, 195405 (2016).

[35] X. Jiang, Y. Cao, K. Wang, J. Wei, D. Wu, and H. Zhu, Surf. Coatings Technology **261**, 327 (2015).

[36] *Springer Handbook of Nanomaterials*, edited by R. Vajtai (Springer, Berlin, 2013).

[37] S. Watcharotone, D. A. Dikin, S. Stankovich et al., Nano Lett. **7**, 1888 (2007).

[38] L. F. Dumée, L. He, Z. Wang et al., Carbon **87**, 395 (2015).

[39] T. Kuila, S. Bose, P. Khanra, A. K. Mishra, N. H. Kim, and J. H. Lee, Biosens. Bioelectr. **29**, 4637 (2011).

[40] Yu. V. Bludov, M. I. Vasilevskiy, and N. M. R. Peres, Europhys. Lett. **92**, 68001 (2011).

[41] F. H. L. Koppens, D. E. Chang, and F. J. García de Abajo, Nano Lett. **11**, 3370 (2011).

[42] G. L. Klimchitskaya, C. C. Korikov, and V. M. Petrov, Phys. Rev. B **92**, 125419 (2015); **93**, 159906(E) (2016).

[43] G. da Gunha Rodrigues, P. Zelenovskiy, K. Romanyuk, S. Luchkin, Ya. Kopelevich, and A. Kholkin, Nature Comm. **6**, 7572 (2015).

[44] Y.-J. Kang, J. Kang, and K. J. Chang, Phys. Rev B **78**, 115404 (2008).

[45] M. Ishigami, J. H. Chen, W. G. Cullen, M. S. Fuhrer, and E. D. Williams, Nano Lett. **7**, 1643 (2007).

[46] N. T. Cuong, M. Otani, and S. Okada, Phys. Rev. Lett. **106**, 106801 (2011).

[47] J. Tang, C. Y. Kang, L. M. Li, W. S. Yan, S. Q. Wei, and P. S. Hu, Physica E **43**, 1415 (2011).

[48] *Handbook of Optical Constants of Solids*, edited by E. D. Palik (Academic, New York, 1985).

[49] A. A. Banishev, H. Wen, J. Xu, R. K. Kawakami, G. L. Klimchitskaya, V. M. Mostepanenko, and U. Mohideen, Phys. Rev. B **87**, 205433 (2013).

[50] M. Bordag, I. Fialkovsky, and D. Vassilevich, Phys. Rev. B **93**, 075414 (2016).

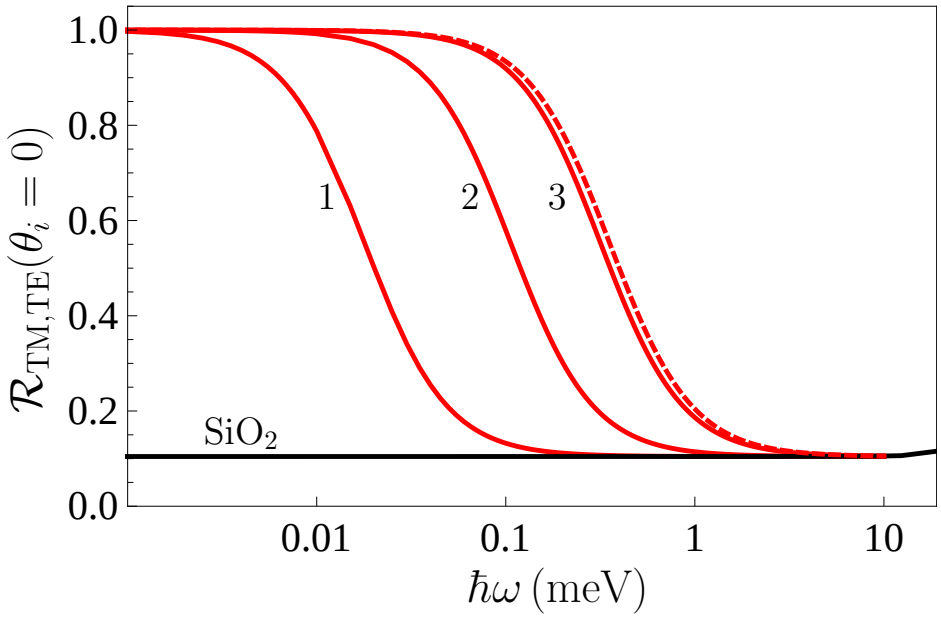

FIG. 1: (Color online) The reflectivities of graphene-coated SiO_2 plates at the normal incidence are shown as functions of frequency at T=300 K by the solid lines 1, 2, and 3 for the mass-gap parameter equal to 0.2, 0.1, and 0.02 eV, respectively. The solid line marked SiO_2 and the dashed line correspond to the cases of an uncoated and coated with a gapless graphene SiO_2 plate.

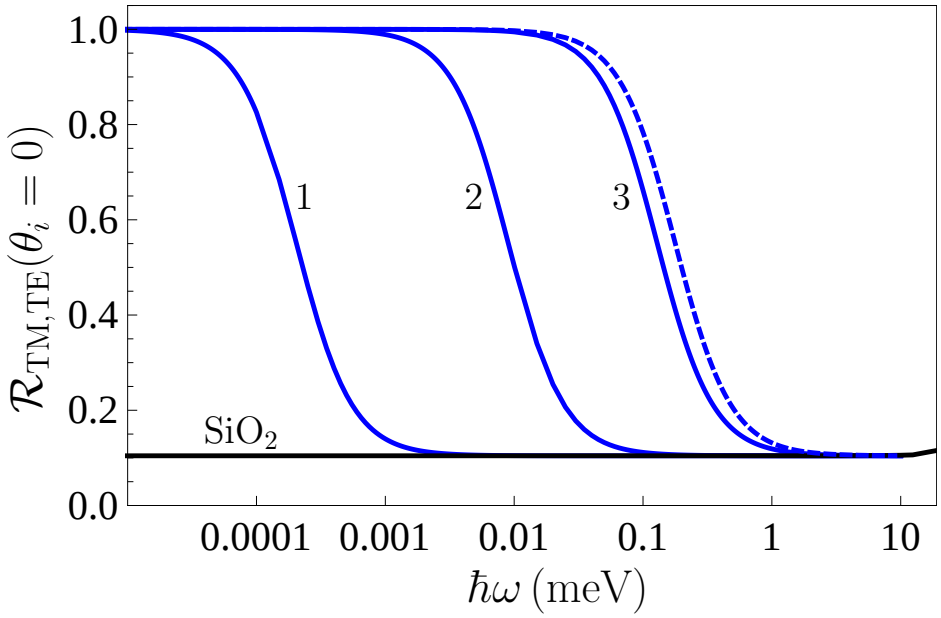

FIG. 2: (Color online) The reflectivities of graphene-coated SiO_2 plates at the normal incidence are shown as functions of frequency at T=150 K by the solid lines 1, 2, and 3 for the mass-gap parameter equal to 0.2, 0.1, and 0.02 eV, respectively. The solid line marked SiO_2 and the dashed line correspond to the cases of an uncoated and coated with a gapless graphene SiO_2 plate.

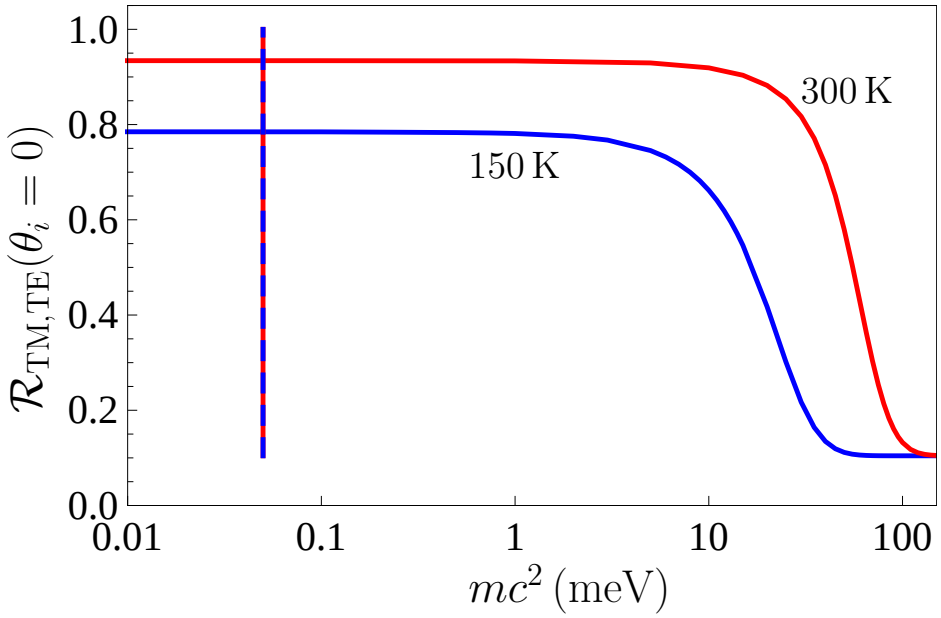

FIG. 3: (Color online) The reflectivities of graphene-coated SiO_2 plates at the normal incidence are shown as functions of quasiparticle mass at $\hbar\omega$=0.1 meV by the solid lines plotted at T=300 K and T=150 K. The overlapping vertical solid and dashed lines indicate the value of mc^2=0.05 meV, where the reflectivity turns into unity at T=300 K and T=150 K, respectively.

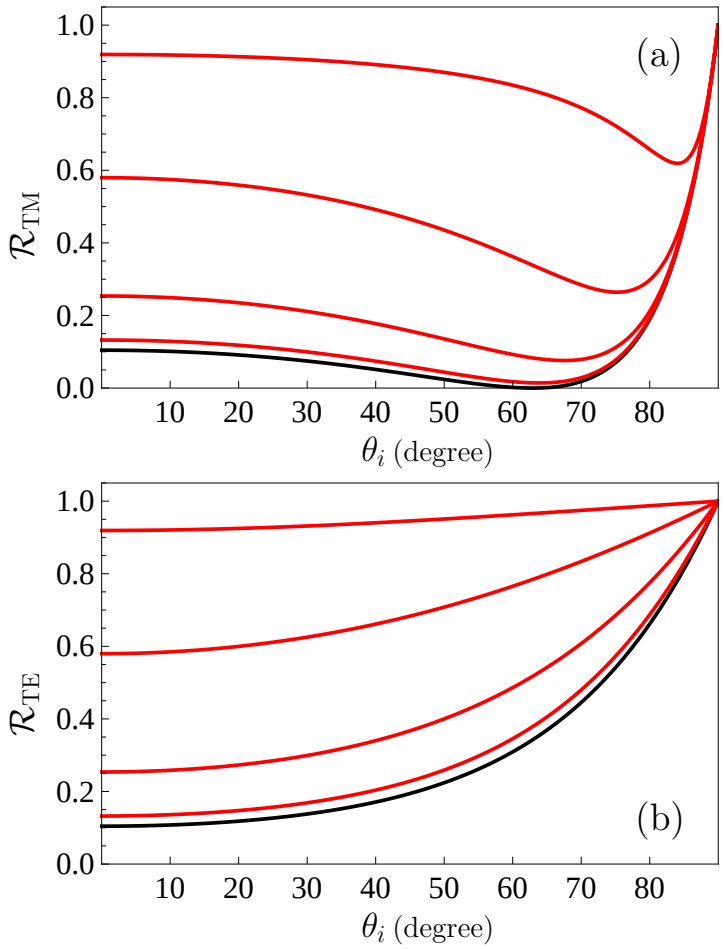

FIG. 4: (Color online) The reflectivities of SiO_2 plates with no graphene coating and coated by gapped graphene with Δ=0.2, 0.15, 0.1, and $\leqslant$0.02 eV are shown as functions of an incidence angle at T=300 K, $\hbar\omega$=0.1 meV by the five solid lines from bottom to top, respectively, for (a) TM polarization and (b) TE polarization of the incident light.

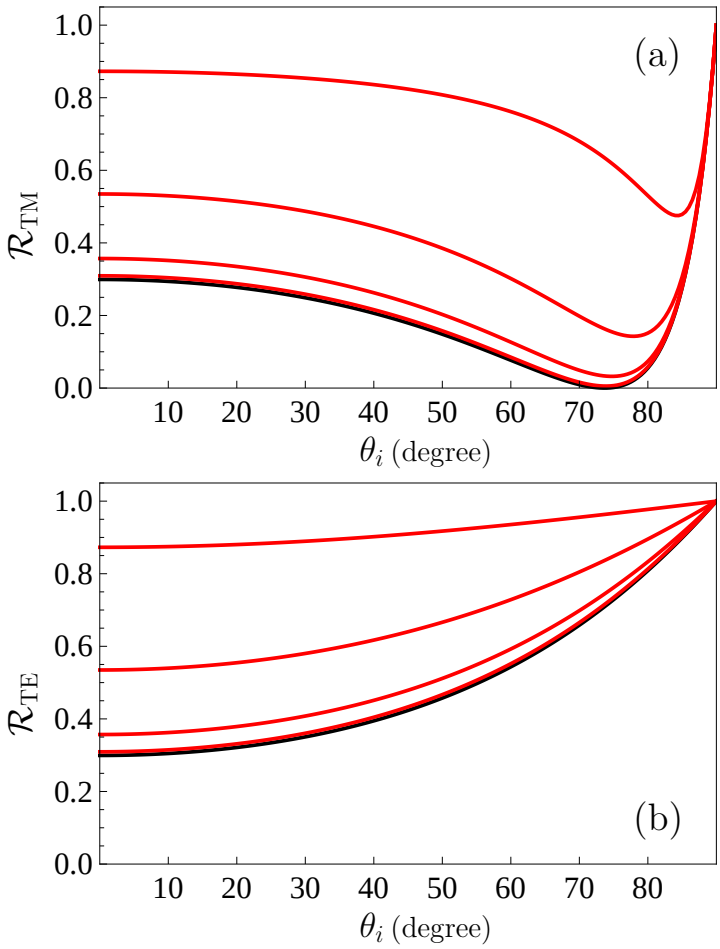

FIG. 5: (Color online) The reflectivities of Si plates with no graphene coating and coated by gapped graphene with Δ=0.2, 0.15, 0.1, and $\leqslant$0.02 eV are shown as functions of an incidence angle at T=300 K, $\hbar\omega$=0.1 meV by the five solid lines from bottom to top, respectively, for (a) TM polarization and (b) TE polarization of the incident light.

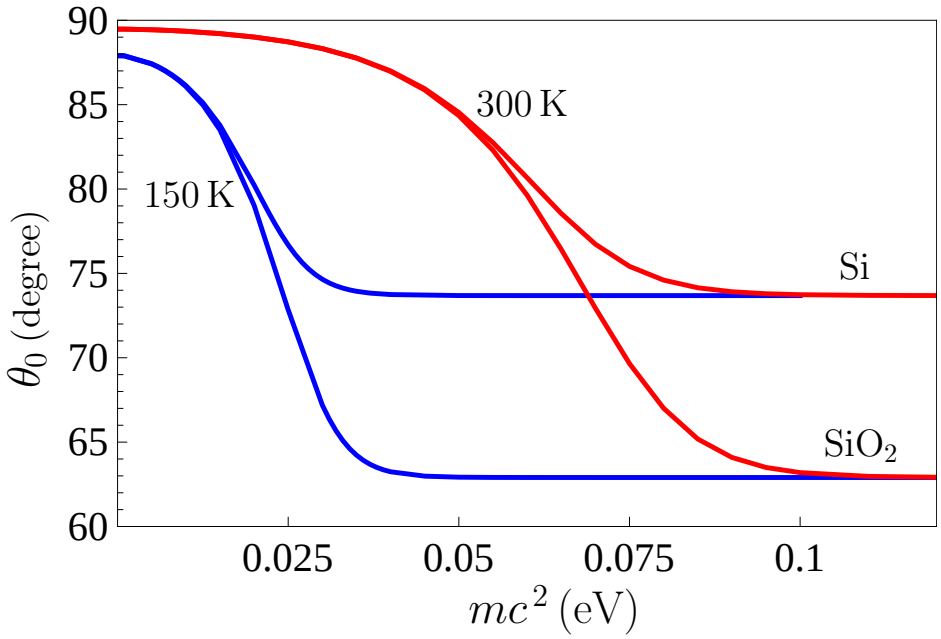

FIG. 6: (Color online) The incidence angles such that the TM reflectivities of graphene-coated Si and SiO_2 plates at T=300K and $\hbar\omega$=0.1 meV take the minimum values, are shown as functions of quasiparticle mass by the top pair of upper and lower lines, respectively. The lower pair of lines presents similar results computed at T=150 K.